JOURNAL OF CATALYSIS **179,** 111–128 (1998)
ARTICLE NO. CA982207

Role of Surface Hydration State on the Nature and Reactivity of Copper Ions in Cu-ZrO_2 Catalysts: N_2O Decomposition

C. Morterra,*,[1] E. Giamello,* G. Cerrato,* G. Centi,† and S. Perathoner†

*Dipartimento di Chimica IFM, Università di Torino, via P. Giuria 7/9, I-10125 Torino, Italy; †Dipartimento di Chimica Industriale, Università di Messina, Salita Sperone 31, 98166 Messina, Italy

Received March 9, 1998; revised June 9, 1998; accepted June 9, 1998

The characteristics of Cu ions loaded in different amounts on ZrO_2 have been studied as a function of the pretreatment conditions (in vacuo, in air, or pure O_2, and after room temperature hydration) by EPR, FTIR of CO adsorption (at 77 K and 300 K), and UV-Vis-NIR diffuse reflectance spectroscopy. The present results indicate : (i) two families of Cu^{II} centres at the surface of oxidized samples; (ii) the easy reducibility of Cu^{II} ions to Cu^{I} ions, and, eventually, to Cu^0, especially in the presence of some surface contaminants and/or when starting from highly hydrated materials; (iii) Cu^{I} centres are easily reoxidized to Cu^{II} by the room temperature action of H_2O, whereas the reoxidation of Cu^0 centres requires the action of O_2 at high temperatures; (iv) the surface situation typical of the starting Cu-ZrO_2 catalysts can be obtained again from reduced catalysts only by the joint action of O_2 at high temperatures (leading to CuO nanoparticles) and H_2O at ambient temperature (redispersing the Cu^{II} species). The stationary and nonstationary catalytic behaviour of Cu-ZrO_2 systems in the decomposition of N_2O at 723 K depends strongly on the pretreatment conditions and can be correlated to the dispersion, oxidation, and hydration state of Cu surface species.

Key Words: **copper; nature of species; zirconia; support for Cu; N_2O decomposition; copper; reoxidation by water.**

INTRODUCTION

Transition metals supported on zirconium oxide have received in recent years an increasing attention as catalytic materials for the interesting surface and reactivity properties obtained when using zirconia as a support. Similarly to TiO_2, zirconium oxide promotes the effective surface spreading of vanadium-oxide (1) and promotes the reactivity of vanadium ions in the reduction of NO in the presence of ammonia and O_2 (2). Iron supported on zirconia shows interesting catalytic properties in the dehydrogenation of olefins (3) and in the hydrogenation of carbon monoxide (4). Kim and Wachs (5) showed that the reactivity of supported Cr-oxide in methanol oxidation is about one order of magnitude higher when supported on ZrO_2 than on other oxides such as SiO_2. The same authors observed that also the activity of molybdenum oxide is promoted by supporting it on zirconia or titania (6). The superior hydrotreating properties of Mo/ZrO_2 catalysts are also well recognized (7–8). Co and Mn oxides supported on zirconia show good properties in 1-butene to butadiene conversion (9) and the promotion effect of zirconium in the catalytic behavior of Co/SiO_2 catalysts for Fisher–Tropsh synthesis has been demonstrated (10). Also the behavior of noble metals may be promoted by dispersion on zirconia with respect to silica or alumina. Mark and Maier (11) showed that ZrO_2 promoted Rh/SiO_2 catalysts are effective for the CO_2 reforming with methane, and Borer *et al.* (12) reported the superior performances of these catalysts for CO hydrogenation. Burch and Loader (13) showed the improved behavior of Rh supported on zirconia for the reduction of NO with hydrocarbons in the presence of O_2.

An interesting class of zirconia supported catalysts is that based on copper oxide. With respect to other supported copper-oxide systems, Cu-ZrO_2 catalysts have been studied in much less detail, despite their promising surface and reactivity properties (14). Zirconia has emerged as a particularly interesting support material for copper catalysts in the synthesis of methanol from either CO/H_2 or CO_2/H_2 (15–19). Cu-ZrO_2 catalysts have interesting reactivity characteristics in the reduction of NO under lean-burn conditions in the presence of both low and high molecular weight hydrocarbons (20–22) and in the NO–CO reaction at low temperatures (23). The behavior of copper ions in the low temperature oxidation of CO is also promoted using zirconia or modified zirconia supports (24–25). Recently, we have shown that, when supporting copper oxide on zirconia, it is possible to obtain better activities in the decomposition of N_2O with respect to other oxide supports (26). In the latter case, the catalytic behavior turns out to be comparable to that of catalysts based on copper ion-exchanged in ZSM-5 zeolite, reported in patent and open literature as very active for this reaction (27–28).

[1] Author to whom correspondence should be addressed: E-mail: morterra@ch.unito.it.

0021-9517/98 $25.00

N_2O contributes significantly to global warming and destruction of ozone layer. As a consequence, antropogenic N_2O emissions, and especially those from combustion and chemical industrial processes, should be reduced by some 80–90% in the near future (29–31).

Water and oxygen are typical major components in the emissions from industrial processes. In the study of the effect of these gas components on the catalytic reactivity of zirconia-based catalysts for N_2O decomposition we noted that the effect on the surface reactivity cannot be explained only in terms of the competitive chemisorption of water at the sites necessary for N_2O decomposition and/or oxygen on the same sites. The presence of these gaseous species is thought to influence directly the nature of surface sites and their intrinsic reactivity (26,32).

The aim of this work is to characterize the nature of copper species in Cu-ZrO_2 catalysts and analyze how it depends on the hydration state of the catalyst and on the conditions of thermal treatments (e.g., in the presence/absence of oxygen). These indications should be compared with the observed effect of water and/or oxygen on the reactivity of Cu-ZrO_2 catalysts in the decomposition of N_2O.

EXPERIMENTAL

Materials

The starting zirconia samples (hereafter referred to as **Z** samples) were prepared following a sol-gel technique (base catalyzed hydrolysis of $Zr(O\text{-iso-}C_3H_7)_4$ diluted in a 1 : 5 volume with ethanol) as reported in more detail in Ref. (25). After ageing (40 min, pH = 10, r.t.) and filtration, the solid was dried at 400 K and then calcined in an air flow up to 773 K using a linear increase of temperature (50°/h) up to the final temperature that was then maintained constant for 4 h. The resulting ZrO_2 phase is microcrystalline, tetragonal (as indicated by XRD data nonreported), and has a mean diameter of the crystalline particles of 18 nm after calcination. The N_2 BET surface area is 93 m^2/g.

On the precalcined Z support, copper was loaded by the incipient wetness method, using dosed amounts of an aqueous solution of $Cu(NO_3)_2$ so as to obtain loading values (expressed as wt% CuO) of about 0.2 and 1, respectively. These samples, hereafter referred to as **CZ*n*** (where ***n*** stands for the CuO loading, i.e., either 0.2 or 1), were air dried, calcined in air at 773 K for 2 h, and then stored in closed vessels. After calcination the surface area of the samples was 92 and 90 m^2/g for the samples with 0.2 and 1% CuO, respectively.

Before all spectroscopic experiments, the "as prepared" samples were vacuum activated at various T_{act} (K) temperatures (see below), and the samples are therefrom designated by the symbol **CZ*n*(T)** (e.g., CZ0.2(473) stands for a Cu/ZrO_2 catalyst, whose CuO loading is 0.2% and that was activated *in vacuo* at 473 K). Whenever the vacuum activation treatment was carried out on CZ catalysts after a previous treatment (e.g., after oxidation, rehydration, or else), no complex symbols will be used to designate the samples, but the operations performed will be explicitly reported both in the text and in the figure captions.

In no phase of the complex physical/chemical treatments performed on CZ samples did XRD data of all CZ*n* samples ever evidence the presence of extra reflexes besides those typical of the ZrO_2 support.

Methods

Before spectroscopic measurements, Z and CZ*n* samples were placed in proper quartz cells (in the form of loose powder for EPR and UV-Vis experiments and as self-supporting pellets ($\sim$20 mg cm^{-2}) for IR experiments) and were activated *in vacuo* in a conventional vacuum line capable of a residual pressure $<10^{-5}$ torr at a temperature between $\sim$300 and 823 K.

Electron paramagnetic resonance (EPR) spectra were obtained both at liquid nitrogen temperature (77 K) and at ambient temperature ($\sim$300 K) with a Varian E-109 spectrometer (X-band), equipped with a dual cavity.

Fourier transform infrared (FTIR) spectra were obtained at 2 cm^{-1} resolution with Bruker spectrophotometers, model IFS 113v or IFS 88, equipped with MCT cryodetector. The spectra of adsorbed species were recorder either at beam temperature, or at a temperature close to that of boiling liquid nitrogen, as reported in the text and figure captions.

In situ UV-Vis-NIR spectra were obtained at ambient temperature in the diffuse reflectance mode, using a Perkin-Elmer spectrophotometer, model Lambda 19.

Catalytic tests were carried out in a quartz fixed-bed reactor equipped with an on-line mass-quadrupole system for the continuous analysis of the feed and of reaction products. Results were corrected to consider overlap in the fragmentation in the mass intensities. Tests were made using 1.0 g of catalyst in the form of particles with diameter of the order of 0.1-mm range and a space-velocity of 4200 h^{-1}. The uniform axial temperature profile of the catalytic bed was monitored using a thermocouple. The feed composition was 1.0% N_2O in He. The following procedure was adopted for the catalytic tests: after calcination and sieving, the catalyst was introduced in the reactor and pretreated *in situ* as indicated in the text. Then the temperature of the reactor was rapidly increased or decreased to 723 K (usually in 10–15 min) feeding a pure He flow to the reactor. When the reactor temperature was stabilised, the feed was switched to the 1% N_2O/He mixture and the outlet composition of the reactor was continuously monitored to determine how the surface reactivity changed in reaching the steady-state behavior.

RESULTS AND DISCUSSION

1. EPR Data

The EPR technique has been employed to monitor the Cu^{II} paramagnetic sites present on CZ*n* catalysts isolated in various redox conditions.

1.1. Reducibility of Cu^{II} Ions

All the "as prepared" samples exhibit an intense EPR spectrum due to cupric ions. Despite the line broadening due to the high surface concentration of cupric ions, the features of a signal with $g_{\|} = 2.30$ and $A_{\|} = 150$ *G* (species A in **Table 1**) are observed for the low loading CZ0.2 sample (**Fig.1a**). The corresponding spectrum for CZ1, although broader and less structured, exhibits the features of species A overlapped with a broad unresolved signal corresponding to clustered Cu^{II} species with the ions in magnetic interaction.

EPR spectra of Cu^{2+}/ZrO_2 catalysts, prepared with the same procedure of the samples analyzed in the present paper, were recently reported by Liu *et al.* (33). Only the spectra of the calcined materials were available (thus comparable with the spectrum in Fig. 1a), but the spin-Hamiltonian parameters reported by Liu *et al.* (33) are quite different ($g_{\|} = 2.38$ and $A_{\|} = 110$ *G*) from those measured in the present case. The discrepancy could be due to the higher copper loading, causing a relatively low resolution of the spectra.

Evacuation at increasing temperature, with progressive dehydration of the sample, causes the decrease of the spectral intensity. At 373 K (spectrum **1b**) the decrease is of some 20% and at 773 K the signal is nearly vanished, due to the gradual reduction of cupric ions. Parallel to the intensity decrease, the resolution of the spectra increases and the signal observed after outgassing at 573 K becomes that of a single Cu^{II} species on ZrO_2 (species B; see **Fig. 1c**). The resolution of the spectrum in Fig. 1c is higher than that observed for several other copper-on-oxide systems

TABLE 1

Spin-Hamiltonian Parameters of Cu^{2+} Ions as a Function of the Thermal or Chemical Treatment of a CZ0.2 Sample

State of the sample	Species	$g_{\|}$	$A_{\circ}$	$g_{\perp}$	$A_{\acute{A}}$
As prepared	A	2.30	150	2.05	Unresolved
Outgassed 570 K	B	2.285	150.0	2.047	18.9
Outgassed 770 K	No Cu^{II}	—	—	—	—
Oxidized	B	2.285	150.0	2.047	18.9
O_2 770 K	C	2.235	160	2.045	20.8
Rehydrated H_2O-R.T.	A	2.30	150	2.05	Unresolved

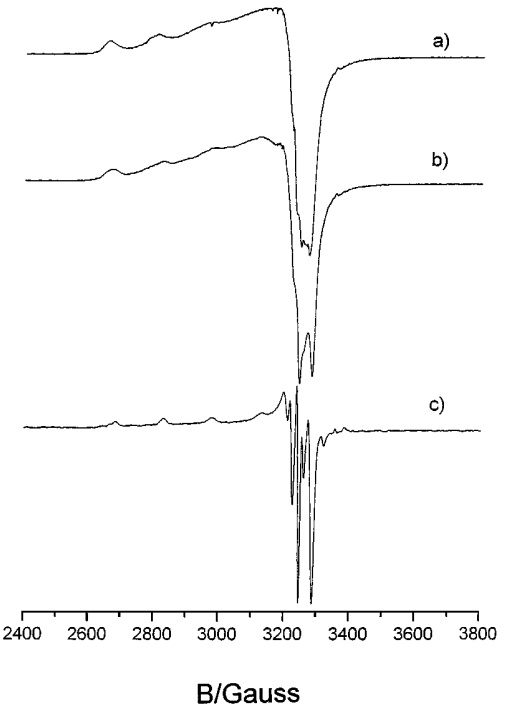

FIG. 1. EPR spectra of CZ0.2 evacuated at 300 K (a), 373 K (b), and 573 K (c), respectively.

(34–35) and is comparable with the resolution observed for the spectra of Cu^{II} ions in zeolites (36). This indicates the presence on the dehydrated system of a single, well-defined and isolated cupric surface complex. The spin-Hamiltonian parameters of the signal have been derived by computer simulation (**Fig. 2**), and are reported in Table 1 (species B).

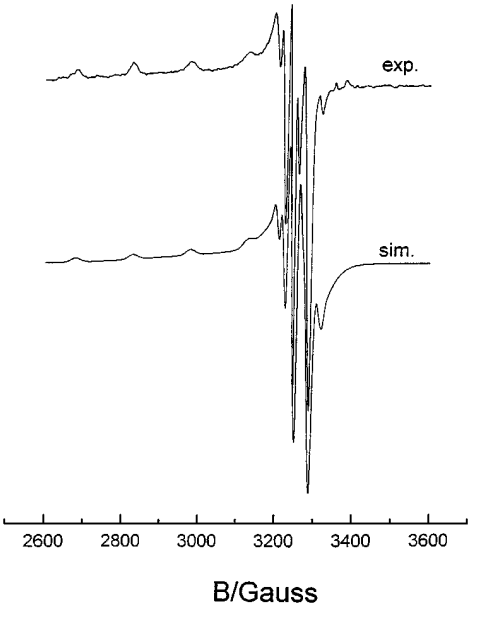

FIG. 2. Computer simulation of the EPR spectrum of the sample CZ0.2(573).

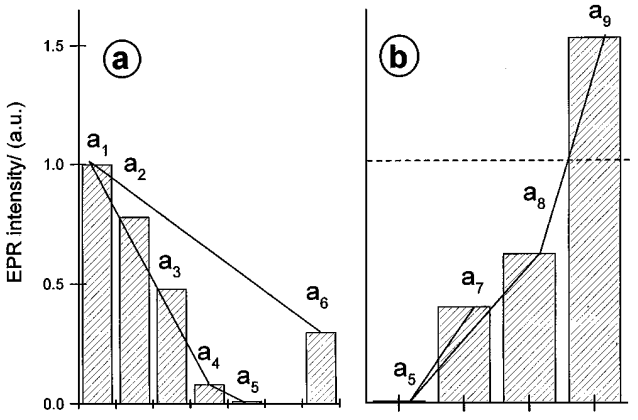

FIG. 3. Integrated intensity of the Cu^{II} EPR spectra of CZ0.2. (**a**) Upon treatment in vacuo at room temperature: "as prepared" sample (a_1); 373 K (a_2); 473 K (a_3); 573 K (a_4); 773 K (a_5); and further, to interaction with CO at RT (a_6). (**b**) The effect of various treatments on the CZ0.2 sample vacuum reduced at 773 K. H_2O adsorption at RT (a_7); oxidation with O_2 at 773 K (a_8); H_2O adsorption at RT after O_2 oxidation at 773 K (a_9).

The EPR spectrum of species B is typical of Cu^{II} ions in axial symmetry. Most probably the symmetry of the environment is distorted octahedral (or square pyramidal), as typical of many cupric systems. From EXAFS and XANES experiments on Cu-ZrO_2 (23) a coordination number of six was found for Cu^{II} ions, in substantial agreement with the present findings.

The considerable reduction of the spectral intensity upon outgassing at increasing temperatures is described in **Fig. 3a**. The graph shows that, after outgassing at 573 K (i.e, in the conditions described by Fig. 1c or Fig.2), only ~8% of the Cu^{II} initially present on the "as prepared" sample remains at the surface. This small residual amount of cupric ions is then nearly eliminated after a further vacuum activation at 773 K.

A considerable reduction of Cu^{II} ions is also observed by contacting at ~300 K the "as prepared" CZ catalysts with a mild reducing agent like carbon monoxide. For instance, in the case of a CZ0.2(300) sample, the amount of Cu^{II} ions is reduced to about 30% of its initial value (see the last column in Fig. 3a), whereas the extent of reduction is somewhat less pronounced in the case of CZ1.0(300) samples (not shown in the figures).

1.2. Reoxidation of Reduced Copper Ions

Reoxidation of a sample vacuum reduced at 773 K has been made by two alternative procedures, the first one being the treatment in molecular oxygen, either at ambient temperature or at high temperature (773 K), and the second one being the contact with water vapour at room temperature. No effect is produced on the cupric ion concentration by contacting the reduced sample with O_2 at room temperature, whereas by contact with O_2 at 773 K a reoxidation occurs (see step a_8 in Fig.3b) leading to an EPR signal of Cu^{II} corresponding to about 60% of the signal initially present in the starting CZ0.2(300) material. (This percentage increases to about 70% for CZ1.0 sample). This implies that either the O_2 treatment at 773 K does not reoxidize to Cu^{II} all of the Cu surface species that were reduced during the vacuum thermal treatment, or not all of the reoxidized Cu^{II} species can be revealed by the EPR technique.

The EPR spectral features of the reoxidized sample (O_2 at 773 K; step a_8 of Fig. 3b) are shown in **Fig. 4b**; it indicates that a new family of cupric ions is now present at the surface (species C in Table 1) beside the already described species B. Two slightly different, but distinguishable, EPR-active isolated Cu^{II} species in axial symmetry, which differ slightly in the coordinative environment, are thus typical of a dehydrated Cu^{II}/ZrO_2 system.

A sample reoxidized in O_2 at 773 K has been submitted to a second series of thermovacuum treatments at the same temperatures of the first pattern. The loss of EPR

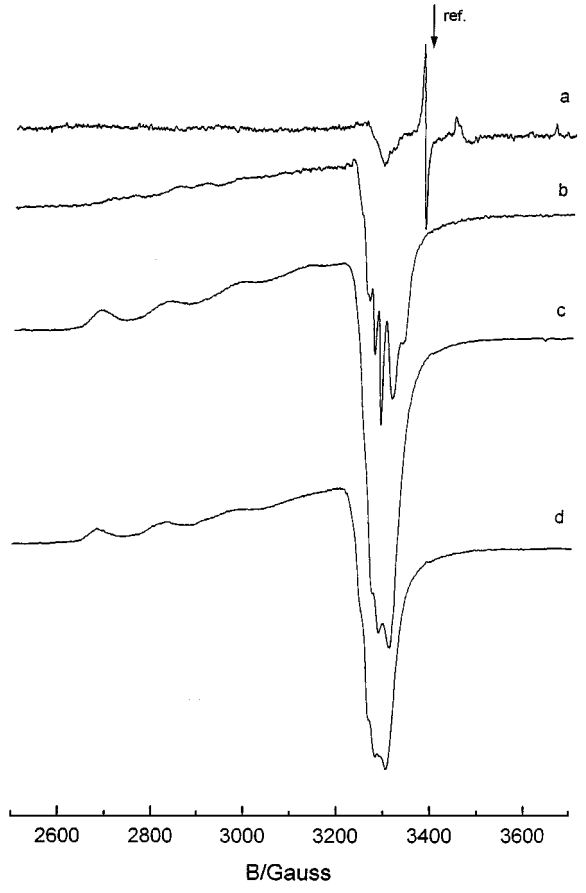

FIG. 4. (**a**) EPR spectrum of CZ0.2(773); (**b**) effect of oxidation in O_2 at 773 K (see a_8 Fig. 3); (**c**) effect of H_2O adsorption at room temperature (see a_7 in Fig. 3); (**d**) effect of H_2O adsorption at RT after O_2 oxidation at 773 K.

intensity observed along the new series of treatments for this dehydroxylated, oxidized material is comparable to that observed for the "as prepared" sample, whose surface is hydroxylated and contaminated by carbonates and hydrocarbonaceous residues (*vide infra*). In particular, the final intensity of the EPR signal after outgassing at 773 K is nearly the same in the two cases.

1.3. Effect of Water on the Redox Behaviour of Copper Ions

Addition of water vapor at room temperature (i.e., the contact with saturated vapor pressure for several minutes) either to the vacuum reduced sample (with Cu^{II} ions practically absent) or to the sample reoxidized in O_2 at 773 K (corresponding to the EPR spectrum of Fig.4b) causes a considerable increase of the Cu^{II} signal suggesting an extensive reoxidation of the system. This is documented in Fig. 3b, steps a_7 and a_9, respectively, and in **Fig. 4,** spectra **c** and **d**, respectively. It is noted that:

(i) In the former case, water addition rises the Cu^{II} content to about 40% of the reference amount initially found on the "as prepared" sample (see the reference horizontal broken line in Fig.3b). This suggests that, during the first activation (dehydration) cycle at $T_{act} = 300$–773 K, an appreciable fraction of Cu^{II}, although not all, was vacuum-reduced to a valence state that is reversible to a plain rehydration at ambient temperature.

(ii) In the second case, water addition leads the Cu^{II} EPR signal to a level that is definitely higher (about 1.5 times) than the initial reference amount. The resulting spectrum is reported in Fig. 4d (amplification of Fig. 4d is lower than Fig. 4c).

In the second case illustrated above the final Cu^{II} spectrum has the same shape and parameters of the "as prepared" material (see Fig. 4c, and the parameters of species A in Table 1). This indicates that on the starting catalyst the Cu situation (i.e., the surface distribution and valence state) is determined by both oxidation *and* hydration state of the system. The fact that, after reoxidation + rehydration, the Cu^{II} signal becomes 1.5 times stronger than on the starting material implies that, on the "as-prepared" starting material, either one or both of the two mentioned parameters (i.e., oxidation, hydration) are appreciably different from that achieved after the *in situ* dehydration–oxidation–rehydration cycle.

2. FT-IR Data

2.1. CO Uptake as a Surface Probe

CO is a weak Lewis base that can interact with coordinatively unsaturated (**cus**) surface sites, forming pure σ-complexes (in d^0 systems) and σ, π-complexes (in d^n systems).

If CO uptake is carried out at ambient temperature (~300 K), the interaction occurs only with the strongest fraction of surface sites, and the CO/strong-site interaction is little perturbed by inductive effects. When in the presence of redox surface species, a drawback of CO adsorption at ~300 K is the mild reducing activity of CO.

If CO uptake is carried out at low temperatures (e.g., 77 K), the reducing activity of CO is usually inhibited, whereas all interactions of the acid–base type may take place. This has the advantage that CO uptake can reveal all surface sites, and the simultaneous disadvantage that the few CO/strong-site interactions are perturbed *via* inductive effects by the abundant CO/weak-site interactions.

2.2. CO Adsorption at ~77 K

Some of the IR spectra recorded at low temperature for the interaction of CO with CZ1.0 samples are reported in **Fig. 5**. Analogous spectra for the support alone are reported, for comparison, in **Fig. 6,** whereas the spectral features of both systems in the ν_{OH} region are shown in **Fig. 7**. The 77 K spectra relative to the interaction of CO with CZ0.2 samples present minor differences and are not described for the sake of brevity.

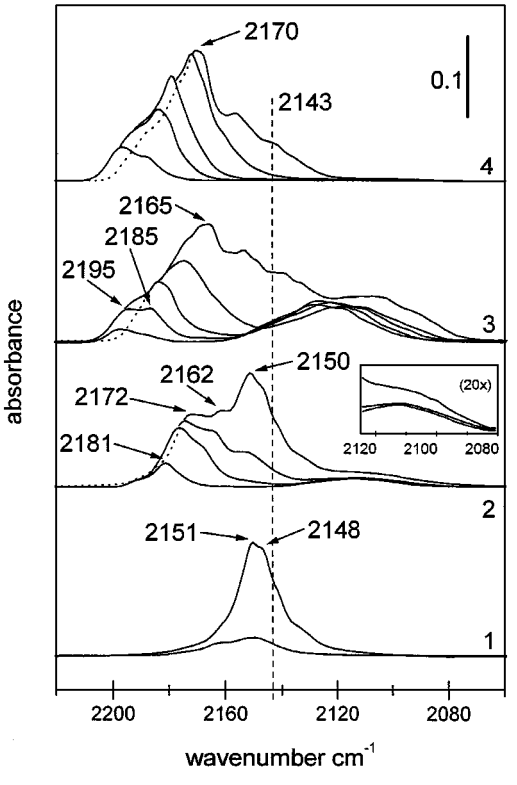

FIG. 5. Absorbance IR spectra of CO adsorbed at ~77 K on CZ1.0(T) samples, under a CO pressure decreasing in the range 4×10^{1}–3×10^{-2} torr. (**1**) $T_{act} = \sim 300$ K; (**2**) $T_{act} = 473$ K; (**3**) $T_{act} = 773$ K; (**4**) after 3, the sample was oxidized with O_2 (60 torr) at 773 K, and the excess O_2 evacuated at ambient temperature.

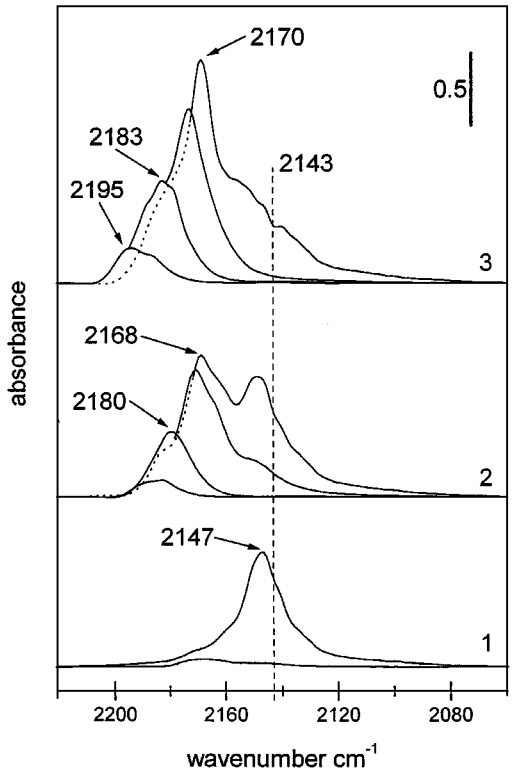

FIG. 6. Absorbance IR spectra of CO adsorbed at ~77 K on zirconia Z(T) samples, under a CO pressure decreasing in the range 4×10^{1}–3×10^{-2} torr. (**1**) $T_{act} = \sim 300$ K; (**2**) $T_{act} = 473$ K; (**3**) $T_{act} = 773$ K.

The spectra of Figs. 5–7 point out the following aspects:

(i) If an "as-prepared" CZ1.0 catalyst is activated *in vacuo* at room temperature (RT), a broad and probably double band forms at ~2155 cm^{-1} at low CO coverages (θ_{CO}). With increasing θ_{CO}, the band grows both in intensity and $\Delta\nu_{1/2}$, and is slightly shifted towards lower wavenumbers (see set 1 in Fig. 5). The position of this band is only slightly higher than that of CO_{gas} (2143 cm^{-1}), indicating either a weak pure σ-donation interaction (in that case it would be a plain H-bonding interaction with surface OH groups), or a σ,π-interaction in which the shifts due to the two contributions almost compensate. The spectral set 1 in Fig. 6, relative to the 77 K CO uptake on pure ZrO_2 activated at RT, indicates that the complex CO absorption at ~2150 cm^{-1} is due to the support component of the CZ1 system and, thus, ascribable to a plain CO/OH interaction of the H-bonding type. This assignment is confirmed by the spectral sets 1 in Fig. 7, showing that CO adsorption brings about the same H-bonding perturbation on the OH spectrum of both CZ1.0(300) and Z(300) systems.

In set 1 of Fig. 5 no spectral components are observed at $\nu > 2160$ cm^{-1} (meaning that no cus cationic sites acting as Lewis acid centres are yet available on CZ1.0(300), as expected of a virtually fully hydrated material), nor at $\nu < 2140$ cm^{-1} (meaning that, despite the presence of Cu, there are no CO species that adsorb with an appreciable π back-donation contribution).

(ii) When the CZ1.0 catalyst is activated *in vacuo* at 473 K, the spectra become far more complex (see set 2 of Fig. 5). At $\nu > 2140$ cm^{-1}, the first species that forms as a function of CO pressure is centered at ~2180 cm^{-1}. On increasing θ_{CO}, another CO component starts appearing at ~2170 cm^{-1}, and the subsequent CO doses bring about the formation of two additional components centered at ~2162 cm^{-1} and ~2150 cm^{-1}, respectively. All of these bands are relative to the σ-coordination of CO to either cus surface cationic sites (Lewis acid sites, $\nu > 2150$ cm^{-1}),

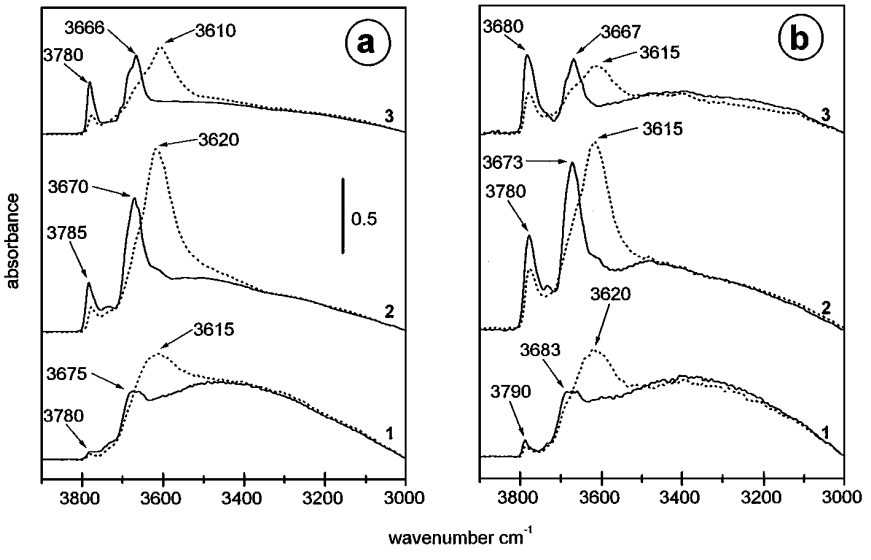

FIG. 7. Absorbance IR spectra in the ν_{OH} spectral region of CZ1.0(T) samples (**a**) and Z(T) samples (**b**). (**1**) $T_{act} = \sim 300$ K; (**2**) $T_{act} = 473$ K; (**3**) $T_{act} = 773$ K. Solid-line curves, background spectra; dotted-line curves, spectra after the allowance of 40 torr CO at ~77 K.

or to surface OH groups ($\nu \approx 2150$ cm^{-1}). The comparison of these bands with those of the spectral set 2 in Fig. 6 and the spectral sets 2 in Fig. 7 confirm that all these CO features are due to the ZrO_2 support (adsorption on cus Zr^{4+} surface sites and on OH groups of the ZrO_2 network).

At $\nu < 2140$ cm^{-1}, the first CO doses form a broad and weak band at $\sim$2115 cm^{-1} that does not change much with increasing θ_{CO} (the band at $\sim$2115 cm^{-1} is better revealed by the blown-up inset to set 2 of Fig. 5). The spectral position of this band and the absence of these features in the spectra of the pure ZrO_2 support indicate the presence on CZ1.0(473) of Cu surface sites capable of chemisorbing CO with an appreciable π back-donation. On the basis of data in the literature (37), the weak band at $\sim$2115 cm^{-1} is ascribed to small amounts of cus Cu^I sites formed by vacuum thermal reduction of the starting Cu^{II} species. EPR data reported in Fig. 3a showed that, after activation at 473 K, the Cu^{II} EPR signal was reduced to $\sim$50% of the original one.

(iii) If the activation of CZ1.0 is carried out *in vacuo* at higher temperatures (namely 773 K; see set 3 in Fig. 5), after CO adsorption an even more complex situation is observed. At $\nu \geq 2150$ cm^{-1}, the first doses of CO favour the formation of a new carbonyl component lying at $\sim$2195 cm^{-1}, which increases in intensity for higher θ_{CO} and becomes clearly double ($\sim$2180 cm^{-1}). For still higher CO pressures, the bands at $\sim$2195 and $\sim$2180 cm^{-1} start shifting with continuity towards lower ν, while another CO component forms with fast increasing intensity at $\sim$2175 cm^{-1} and eventually reaches $\nu_{max} \approx 2170$ cm^{-1}. Comparison with set 3 of Fig. 6 indicates that all of these CO bands, due to a very complex system of Lewis acid sites produced during the high temperature activation, are due to the ZrO_2 support (38). The CO band at $\sim$2150 cm^{-1} (due to H-bonded CO) shows a very low intensity now, due to the high surface dehydration achieved, and is mainly due to OH groups belonging to the ZrO_2 support, as demonstrated by Fig. 6 (set 3) and Fig. 7 (sets 3). In the ν_{OH} spectral region, the presence of Cu brought about only an appreciable change in the relative intensity of the bands due to terminal OH groups ($\sim$3780 cm^{-1}) and bridging OH groups ($\sim$3670 cm^{-1}), typical of the ZrO_2 support (39); it is inferred that the CuO moiety anchors more favourably to the ZrO_2 support through the terminal OH groups.

At $\nu < 2150$ cm^{-1}, a broad band centred at $\sim$2115 cm^{-1} forms at the lowest θ_{CO}, and under increasing θ_{CO} does not change appreciably in intensity, while keeps moving to lower ν with continuity. This broad band is not present in the spectra of pure ZrO_2 and is thus confirmed to be due to CO adsorbed onto Cu^I sites. The broad band due to CO/Cu^I complexes is present on CZ1.0(773) at frequencies rather different from those observed on CZ1.0(473), indicating that the spectral features of these complexes depend also on the conditions of the activation treatment. The position of the $\sim$2115 cm^{-1} band varies much with CO coverage, and this does not allow a convenient use of the spectra at 77 K to follow the spectral changes of the CO/Cu^I complexes with activation conditions. For this reason some CO spectra obtained at ambient temperature will be presented in a following section.

The intensity of the CO/Cu^I band formed on CZ1.0(773) is much higher than that formed on CZ1.0(473); it is so deduced that the vacuum treatment at high temperature brought about an extensive reduction of the copper species. EPR spectra indicated that, in these conditions virtually no EPR visible Cu^{II} remains in Cu/ZrO_2 catalysts. Moreover, the CZ1(773) sample exhibited an appreciable darkening from light grey to dark brown, suggesting that the vacuum reduction process proceeded beyond the Cu^I level and led to the formation of some Cu^0 centres. CO uptake at 77 K does not yield any additional band(s) to be specifically ascribed to CO/Cu^0 complexes (band(s) at $\nu < 2000$ cm^{-1} would be expected (37,40)), and this confirms that CO hardly adsorbs at all on supported Cu^0 centres (40).

(iv) If the activation of CZ1.0 is carried out at 773 K in an oxidising atmosphere, or the vacuum activation at 773 K is followed by an oxidation step 773 K, CO uptake at 77 K leads to the spectra of set 4 of Fig. 5.

At $\nu \geq 2150$ cm^{-1}, most of the spectral features relative to the ZrO_2 component are still present, meaning that the dehydration stage achieved by the catalyst remained almost the same, so that the concentration of the various families of Lewis acid sites and of the OH groups capable of H-bonding CO remained virtually unchanged. But at $\nu < 2150$ cm^{-1} the broad absorption lying at $\sim$2115 cm^{-1} and ascribed to Cu^I/CO complexes is now totally absent. This indicates that the oxidising treatment at 773 K eliminated entirely the surface Cu^I sites and confirms that at 77 K CO has no reducing activity towards Cu^{II} but yields only interactions of the acid/base type. The virtual coincidence at $\nu > 2140$ cm^{-1} of the spectra in sets 3 and 4 of Fig. 5 confirms that, even at 77 K, no CO uptake occurs at a spectroscopically observable level on Cu^{II} sites.

During the oxidising treatment at 773 K, the CZ1.0 sample lost the dark colour acquired during the vacuum thermal treatments and recovered the starting pale grey colour, suggesting the reoxidation to Cu^{II} also of Cu^0 centres. EPR data reported in Fig. 3b (step a_8) showed that, after oxidation at 773 K of a CZ0.2(773) sample, the Cu^{II} signal recovered only $\sim$60% of the original intensity. The complete oxidation to Cu^{II} suggested by CO IR data at 77 K so indicate that, after a plain oxidation at 773 K (with no rehydration), a large fraction of the Cu^{II} species formed are in a EPR silent form, probably in the form of surface dispersed CuO particles (41).

(v) If, after a vacuum activation at 773 K (and the parallel $Cu^{II} \rightarrow Cu^I$, Cu^0 reduction process discussed above), CZ1.0(773) is thoroughly rehydrated at ambient temperature (note that in these conditions the sample remains dark in colour) and then is further dehydrated at ambient

temperature, CO adsorption at ~77 K yields a spectral pattern indistinguishable from that of set 1 in Fig. 5, in which only a H-bonding interaction with OH groups of the ZrO_2 support is observed. This indicates that all of the Cu^I centres formed by vacuum thermal reduction are reoxidized to Cu^{II} by water vapour, whereas Cu^0 centres most likely remain unaffected. EPR data indicated that, in this conditions, about 60% of the original Cu^{II} signal is recovered.

2.3. CO Adsorption at RT

(A) The "as-prepared" samples. The first treatment considered is the vacuum activation at increasing temperatures of an "as-prepared" sample. This treatment mimics the activation cycles normally carried out on real catalysts prior to catalytic reaction.

The IR background spectra reported as curves 1,2,5 in **Fig. 8** show that the starting CZ1.0 catalyst is heavily contaminated with surface carbonate-like species deriving from the exposure to the atmosphere (spectral region 1700–900 cm^{-1} (42)) and that vacuum treatments at T_{act} as high as 773 K (i.e., the highest activation temperature considered in this work) reduce drastically the contamination but are not sufficient to eliminate it entirely. The spectra in Fig. 8 indicate that CZ*n* samples are also abundantly contaminated with hydrocarbonaceous residues deriving from the preparation and post-preparation steps (bands in the 3000–2750 cm^{-1} interval) and that during the thermal dehydration process the contaminants are decomposed *in vacuo* at ~573 K (see inset **b** to Fig. 8). The vacuum pyrolysis of $(CH)_n$ residues certainly enhances the reducing potentiality of the medium in which the "as prepared" catalysts are activated.

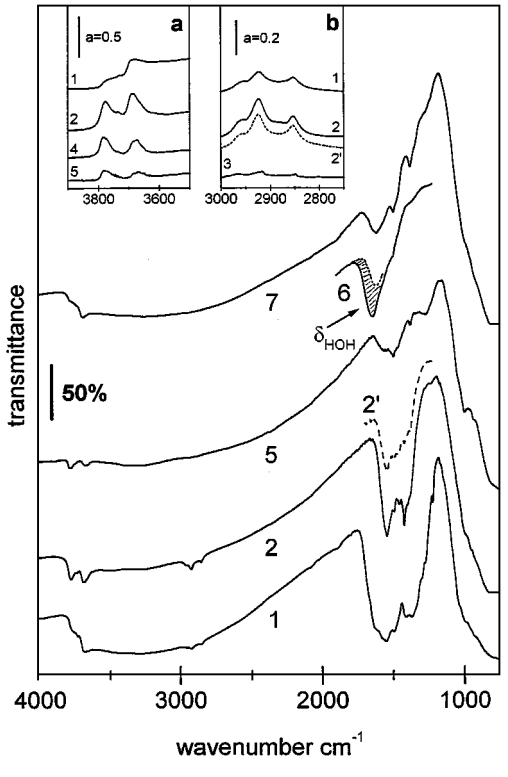

FIG. 8. Whole-range transmittance IR background spectra (and, in the insets, absorbance spectral segments in the ν_{OH} range (**a**) and in the ν_{CH} range (**b**)) of CZ1.0(T) samples. (**1**) T_{act} = ~300 K; (**2**) T_{act} = 473 K; (**2′**) spectral segment of the CZ0.2(473) sample, inserted for comparison; (**3**) T_{act} = 573 K; (**4**) T_{act} = 673 K; (**5**) T_{act} = 773 K; (**6**) after 5, the system was thoroughly rehydrated at ~300 K; (**7**) as for 6, after evacuation at ~300 K for 1 h.

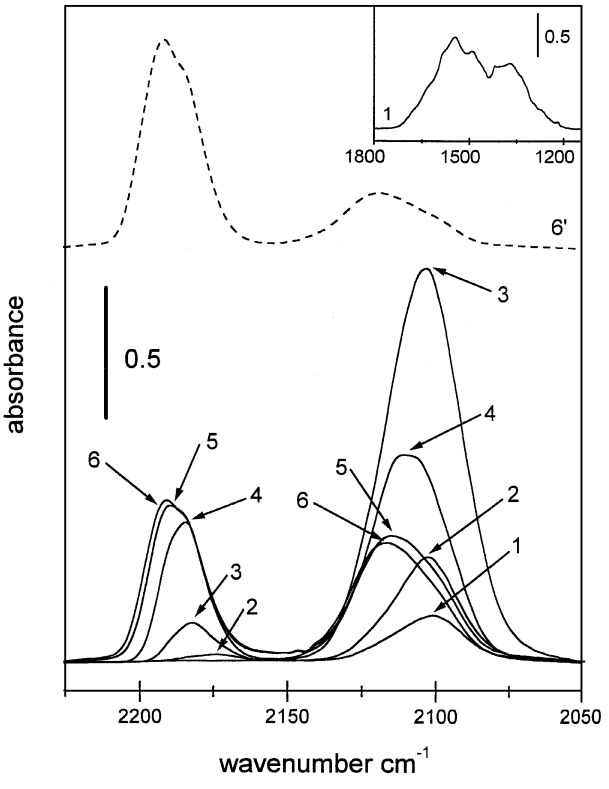

FIG. 9. Absorbance IR spectra of CO adsorbed at ~300 K on "as-prepared" CZ1.0(T) samples, under a CO pressure of 100 torr. (**1**) T_{act} = ~300 K; (**2**) T_{act} = 373 K; (**3**) T_{act} = 473 K; (**4**) T_{act} = 573 K; (**5**) T_{act} = 673 K; (**6**) T_{act} = 773 K; (**6′**) CZ0.2(773), inserted for comparison. Inset: absorbance differential spectral segment of surface carbonates formed by contact with CO at ~300 K on CZ1.0(300).

The IR spectra of CO (100 torr) adsorbed at ambient temperature on an "as prepared" CZ1.0 sample vacuum activated at increasing temperatures are reported in **Fig. 9**. The spectral region at $\nu > 2150$ cm^{-1} concerns CO uptake on cus Zr^{4+} centres sufficiently strong as Lewis acid sites to chemisorb CO at ambient temperature and monitors the surface dehydration degree attained, as well as the fraction of ZrO_2 surface that was not covered by copper (e.g., compare curve 6, relative to CZ1.0(773), and curve 6′, relative to CZ0.2(773)). The spectral region at $\nu < 2150$ cm^{-1} concerns CO uptake on Cu^I surface sites and monitors the fraction of ZrO_2 surface that was covered by copper as well as the degree of occurrence of the $Cu^{II} \rightarrow Cu^I$ reduction

reaction. It has to be considered that, in this case, part of the $Cu^{II} \rightarrow Cu^{I}$ reduction is caused by the RT contact with CO, as was shown by EPR data (Fig. 3a) and as indicated by the fact that bands due to Cu^{I}/CO surface complexes form already on CZ1.0(300), whereas at 77 K no Cu^{I}/CO bands formed at $\nu < 2140$ cm^{-1}. The partial reduction of Cu^{II} upon contact with CO at RT is also indicated by the differential spectrum in the inset to Fig. 9, showing that new carbonate-like species are formed, in addition to the abundant carbonate contaminants already present on the "as-prepared" catalysts. The amount of carbonates formed upon contact with CO at RT (that monitors the ambient temperature reducibility by CO) will decrease fast on CZ1.0 samples vacuum activated at increasing temperatures, and eventually will become null on CZ1.0(673).

The complex band due to Cu^{I}/CO complexes increases first and then declines. This indicates that surface Cu^{I} centres are formed, first at the expense of Cu^{II} ones (the decline of the latter species was clearly shown by EPR spectra) and then Cu^{I} surface centres are gradually eliminated, most likely by a further reduction to Cu^{0}. The darkening of the sample pellet suggests that a $Cu^{I} \rightarrow Cu^{0}$ reduction reaction does actually occur upon vacuum treatment at $T_{act} \geq 650$ K, while the lack of formation of carbonates by CO contact on CZ1.0 samples treated at $T_{act} \geq 650$ K indicates that the reduction to Cu^{0} is indeed due to the vacuum thermal treatment and not to the action of CO at RT.

The band due to Cu^{I}/CO complexes shown in Fig. 9 is clearly double, as also shown by the spectral simulations reported in **Fig. 10**. At low dehydration stages ($T_{act} = 300$–473 K) a spectral component centered at ~2100 cm^{-1} and asymmetric on the high wavenumber side is by far dominant and grows fast with the activation temperature, whereas at high dehydration stages ($T_{act} = 573$–773 K) a second component centered at ~2120 cm^{-1} grows and dominates over a residual component centered at lower wavenumbers. Computer spectral simulations of Fig. 10 and the relevant spectral data in Table 2 show that: (i) the evolution of the Cu^{I}/CO band envelope does not vary appreciably with Cu loading (compare sections **a** and **b** of Fig. 10 and Table 2); (ii) the main spectral features of the two Cu^{I}/CO components (ν_{max}, $\Delta\nu_{1/2}$, as well as the percent gaussian character, not reported) do not change much with the activation temperature. This indicates that the spectral properties of cus Cu^{I} centres (i) do not depend on the overall Cu concentration and (ii) do not change with continuity on dehydration. Two discrete families of Cu^{I} centres exist in all cases, in proportions that vary with the activation temperature. Moreover, the virtually constant spectral position of the two Cu^{I}/CO components with decreasing overall surface concentration of Cu^{II} species, first, and then of Cu^{I} species indicates that the properties of Cu^{I}_{cus} sites do not depend appreciably on the average oxidation degree of surface copper. The low frequency Cu^{I}/CO component can be thus

TABLE 2

Spectral Features of CO/Cu^{I} Complexes Formed at ~300 K at the Surface of CZn (T) Catalysts

1% Cu-ZrO_2	ν_{max} (cm^{-1})	$\Delta\nu_{1/2}$ (cm^{-1})	Relative intensity (% absorbance)
298 K	2100.6	22.9	83
	(2117.3)	(18.4)	(17)
473 K	2103.5	28.1	94
	2122.3	15.0	6
573 K	2102.7	24.7	54
	2116.3	23.2	46
673 K	2103.5	25.6	51
	2120.2	21.8	49
773 K	2101.7	20.9	34
	2120.2	22.3	66
0.2% Cu-ZrO_2	ν_{max} (cm^{-1})	$\Delta\nu_{1/2}$ (cm^{-1})	Relative intensity (% absorbance)
298 K	2101.1	32.9	100
473 K	2103.4	22.7	79
	2119.4	21.93	21
573 K	2103.5	19.9	55
	2117.9	19.9	45
673 K	2106.6	27.4	66
	2120.5	24.5	34
773 K	2105.1	25.6	43
	2122.7	21.9	57

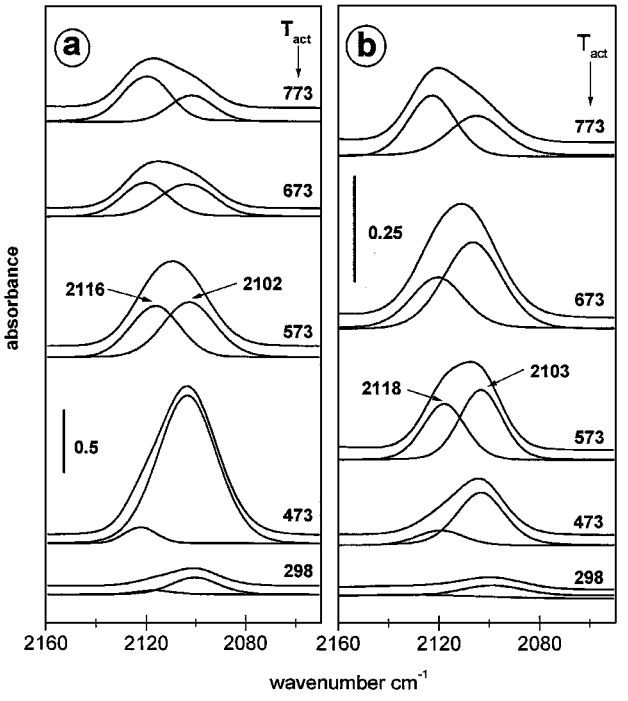

FIG. 10. Computer spectral simulation of the bands formed by the adsorption of CO (100 torr) at ~300 K on "as prepared" CZ1.0(T) samples (**a**) and "as prepared" CZ0.2(T) samples (**b**). T_{act} (K) are as reported on the curves.

thought of as typical of the hydrated CZn catalysts (or of the hydrated parts of the catalyst surface), whereas the high frequency Cu^I/CO component would be typical of the dehydrated (portions of the) catalysts.

An upwards frequency shift of the ν_{CO} mode, brought about by the dehydration process, may mean either an increase of the σ contribution to the Cu-CO bond, or a decrease of the π back-donation contribution. As the two Cu^I/CO adspecies do not exhibit significant differences of resistance to evacuation (i.e., of bond strength), it is difficult to understand what contribution actually changes with the varying surface hydration degree. A recent work on Cu/zeolite systems tends to ascribe to the σ component of the Cu^I-CO bond a decisive role in determining the CO stretching frequency (43).

(B) Sample rehydration. The assignment proposed for the two Cu^I/CO adspecies is confirmed by the spectral pattern reported in **Fig. 11** and by the spectral simulations in **Fig. 12**, relative to the stepwise addition of small water doses on a CZ1.0(773) catalyst onto which CO has been adsorbed (curve 1, the high frequency Cu^I/CO component at $\sim$2120 cm^{-1} dominates, in view of the high dehydration attained). The first water doses bring about first a fast decline of the $\sim$2120 cm^{-1} component and an increase of the low frequency component centered at $\sim$2100 cm^{-1} (see curves 2, 3). Parallel to the increase of the $\sim$2100 cm^{-1} component there is the appearance of another CO component centered at even lower frequency ($\sim$2080 cm^{-1}; see curves 4, 5) that was not present during the dehydration steps. The allowance of further water doses tends to enhance the relative intensity of the $\sim$2080 cm^{-1} component (curve 6), and eventually the overall intensity of the whole Cu^I/CO band envelope declines (curves 7, 8). These spectra can be interpreted in the following way: the first water doses cause a rehydration of the catalyst, and the high wavenumber Cu^I/CO adspecies (typical of the dehydrated system) are transformed into the low wavenumber Cu^I/CO adspecies (typical of the hydrated system). With increasing water pressure, another Cu^I/CO adspecies characterised by a further lowered ν tends to form ($\nu_{max} \approx 2080$ cm^{-1}), due to the introduction of water molecule(s) in the coordination sphere of (some of) the Cu^I/CO complexes. This phenomenon is not unknown at the surface of supported metal and/or metal oxide systems. It is recalled that a similar effect of hydration on the spectral features of CO adsorbed on a Cu-ZSM-5 catalyst was reported by Kapteijn *et al.* (44). Miessner *et al.* (45) observed similar results by adsorbing CO on Cu^I-Y-zeolites. Moreover, the small downward shift of the

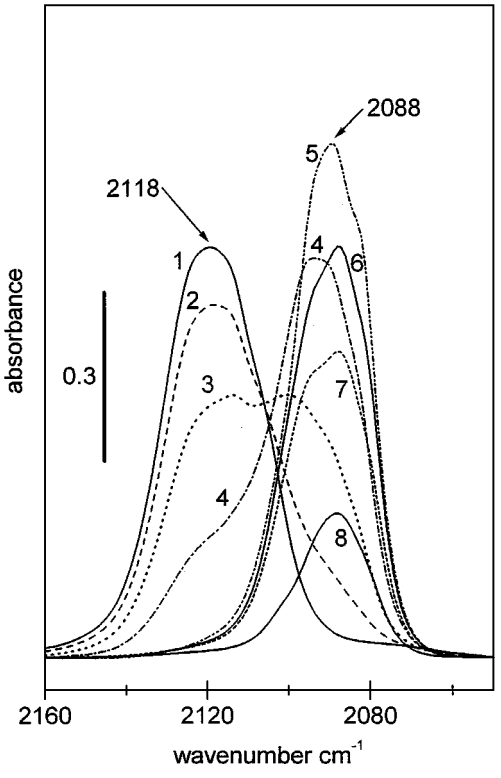

FIG. 11. (**1**) absorbance IR spectrum of CO adsorbed at $\sim$300 K on CZ1.0(773) (100 Torr CO were equilibrated, and then evacuated to 10^{-3} Torr. Only the Cu/CO spectral region is shown, as the Zr/CO adspecies are reversible at $\sim$300 K); (**2**)-(**8**) on pre-adsorbed CO, successive doses of water vapour were allowed (equilibrium P_{H2O} in the $\sim 10^{-1}$–10^{1} Torr range).

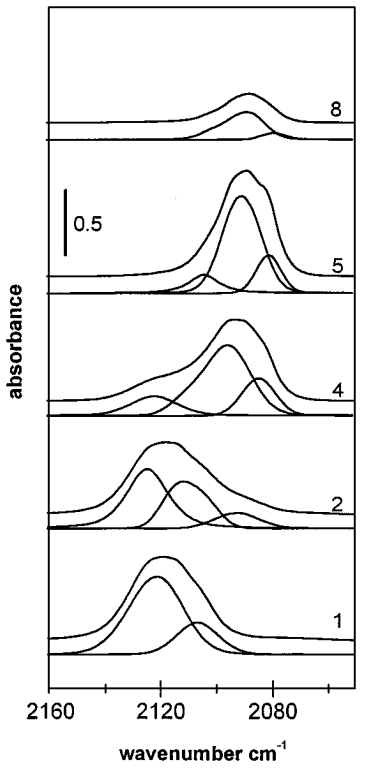

FIG. 12. Computer simulation of some of the Cu/CO curves of Fig. 11. (The numbers marked on the curves correspond to those reported in Fig. 11.)

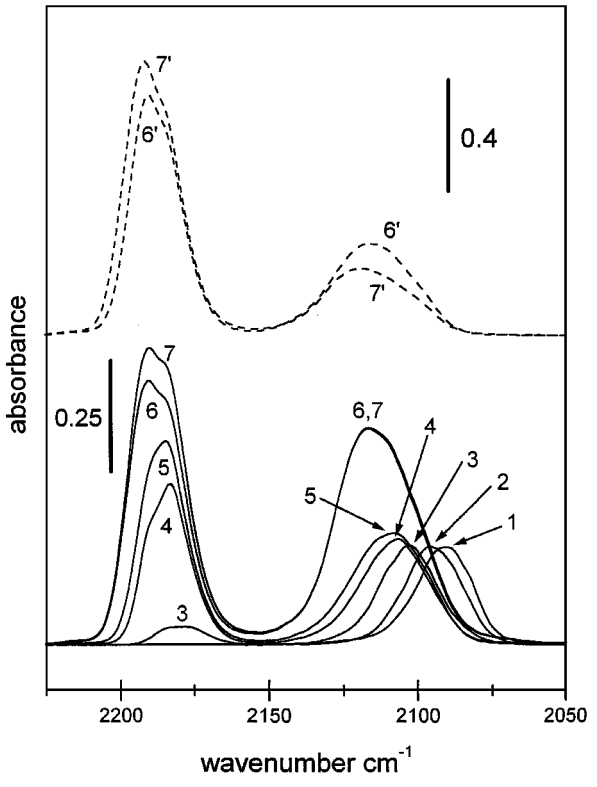

FIG. 13. Absorbance IR spectra of 100 torr CO adsorbed at ~300 K on a CZ1.0 sample first vacuum activated at 773 K (i.e., CZ1.0(773)), and then thoroughly rehydrated at ~300 K and further vacuum activated in various conditions. The temperatures (K) of the second activation pattern are as follows: (**1**) $(T_{act})_{II} = \sim 300$ K, 5 min; (**2**) $(T_{act})_{II} = \sim 300$ K, 60 min; (**3**) $(T_{act})_{II} = 373$ K; (**4**) $(T_{act})_{II} = 473$ K; (**5**) $(T_{act})_{II} = 573$ K; (**6**) $(T_{act})_{II} = 673$ K; (**7**) $(T_{act})_{II} = 773$ K. Upper broken curves refer to a CZ0.2 sample treated in the same way and inserted for comparison: (**6′**) $(T_{act})_{II} = 673$ K; (**7′**) $(T_{act})_{II} = 773$ K.

ν_{CO} mode ($\Delta\nu_{CO} \approx -20$ cm^{-1}) suggests that only one water molecule is inserted in the aquacarbonyl complexes (45).

(C) Rehydrated samples (water reoxidation). In the section devoted to CO adsorption at ~77 K it was reported that, after hydration at RT, no Cu^I surface sites remain available for CO uptake, confirming that the reoxidation of Cu^I sites by water action is complete. **Figure 13** reports, for a rehydrated CZ1.0(773) sample, the spectra of CO adsorption at RT during a further dehydration pattern. It indicates that: (i) after a plain evacuation at ambient temperature a limited reduction is again produced by the contact with CO at RT. In fact, in curve 1, the Cu^I/CO band does not have null intensity; (ii) as long as there is excess water at the surface (as shown, for instance, by the background spectrum 6 in Fig. 8) the Cu^I/CO band is centered at ~2080 cm^{-1}, due to the water ligand in the coordination sphere of the Cu^I/CO complexes. Then the band moves to ~2100 cm^{-1}, the position typical of Cu^I/CO complexes on hydrated catalysts, but with no water molecules in the coordination sphere; (iii) with increasing the dehydration temperature, the $Cu^{II} \rightarrow Cu^I$ reduction process occurs again, and the overall intensity of the Cu^I/CO band increases while the spectral position moves towards ~2120 cm^{-1} (i.e., the spectral position typical of a dehydrated catalyst); (iv) at $T_{act} \geq 650$ K the overall intensity of the Cu^I/CO band does not decrease as it did on the "as-prepared" catalyst during the first activation cycle, meaning that on the rehydrated and water-reoxidized CZ1.0 system no further reduction of Cu^I to Cu^0 occurs to an appreciable extent, although this is not observed in all cases (for instance, the upper curves in Fig. 13 indicate that, in a CZ0.2 sample, the second dehydration pattern did actually yield a further Cu^I - Cu^0 reduction).

(D) O_2-reoxidized samples. The last treatment pattern to be considered in this section is the vacuum activation at increasing temperatures of a CZ1.0(773) sample that, after the vacuum treatment at 773 K, was oxidized with O_2 at 773 K. With this oxidizing treatment the sample recovers the original pale gray colour. EPR spectra showed that, in these conditions, a Cu^{II} signal corresponding to ~60% of the original signal is obtained, whereas CO spectra at ~77 K showed that, in these conditions, no Cu^I sites available for CO uptake remain at the surface. CO adsorption at RT on the reoxidized–reactivated sample yielded the spectra reported in **Fig. 14**. Appreciable differences with respect to the spectra of the "as-prepared" material (Fig. 9) and of the rehydrated material (Fig. 11) are noted and can be summarized as follows:

(i) The bands of CO adsorbed on cus Zr^{4+} sites ($\nu_{CO} > 2160$ cm^{-1}) reach almost immediately their maximum intensity, as the oxidation process at 773 K did not cause an appreciable rehydration (but for the unavoidable minor contamination deriving from the prolonged use in static conditions of a conventional high-vacuum system). Still, the maximum intensity of the Zr^{4+}/CO band envelope is far lower than that reached, after vacuum treatment at 773 K, on the "as-prepared" material or, even more evident, on the rehydrated material. Since the dehydration level attained is not different from that of the other materials (OH spectra fairly similar to those of curves 4 and 5 of the inset **a** to Fig. 8 were obtained), it is inferred that the first activation cycle at up to 773 K and/or the subsequent oxidation at 773 K produced a different distribution of the Cu moiety over the support. A lower portion of the ZrO_2 support is now free from Cu and, when dehydrated, is available for an acid–base Zr^{4+}_{cus}/CO interaction at RT.

(ii) No matter what the vacuum activation temperature, CO bands at $\nu < 2150$ cm^{-1} due to Cu^I/CO complexes have the maximum constantly centered at ~2120 cm^{-1}, as expected of a system that remained, after reoxidation, highly dehydrated.

(iii) CO bands at $\nu < 2150$ cm^{-1} show that, unlike what observed at ~77 K, at RT Cu^I/CO complexes form with great intensity already after a plain evacuation at ambient

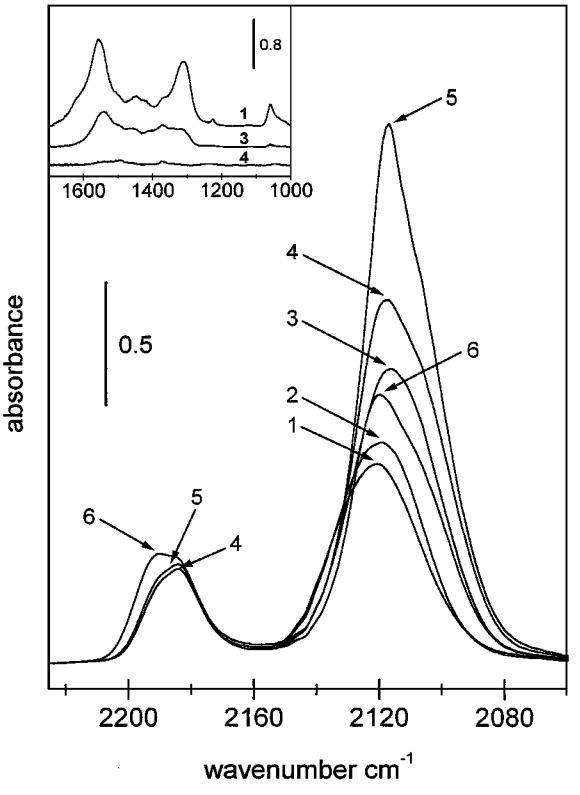

FIG. 14. Absorbance IR spectra of 100 Torr CO adsorbed at ~300 K on a CZ1.0 sample first vacuum activated at 773 K (i.e., CZ1.0(773)) and then oxidized with O_2 (60 Torr) at 773 K and further vacuum activated in various conditions. The temperatures (K) of the second activation pattern are as follows: (**1**) $(T_{act})_{II} = \sim 300$ K, 60 min; (**2**) $(T_{act})_{II} = 373$ K; (**3**) $(T_{act})_{II} = 473$ K; (**4**) $(T_{act})_{II} = 573$ K; (**5**) $(T_{act})_{II} = 673$ K; (**6**) $(T_{act})_{II} = 773$ K. Inset: absorbance differential spectral segment of surface carbonates formed, by contact with CO at ~300 K, on the samples treated as reported above at ~300, 473, and 573 K, respectively.

temperature. This indicates that the reducibility with CO to Cu^{I} of the Cu^{II} phase formed upon reoxidation is much higher than that observed on the "as-prepared" material; this is confirmed by the large amount of carbonates formed upon contact with CO (see inset to Fig. 14; note that the ordinate scale is about one half of that of the inset to Fig. 9). The easy reducibility of Cu^{II} to Cu^{I} by contact with CO will remain up to activation temperatures as high as ~673 K.

(iv) The reducibility to Cu^0 of the reoxidized Cu species is definitely lower. In fact, the band of Cu^{I}/CO complexes keeps growing to very high intensities after activation at temperatures as high as 673 K, and a decline of the Cu^{I}/CO band will be observed only after vacuum treatment at 773 K (see trace 6 in Fig. 14). The residual intensity of the Cu^{I}/CO band will remain fairly high also after the treatment at 773 K, confirming the EPR datum of a lower vacuum reducibility of Cu^{II} in the Cu phase(s) obtained by reoxidation with O_2 at high temperatures. The later and lower extent of the $Cu^{I} \rightarrow Cu^0$ reaction on reoxidized CZn samples is certainly ascribable, in part, to the absence on reoxidized samples of surface hydrocarbonaceous contaminants, whose vacuum pyrolysis at $T_{act} \geq 573$ K is partly responsible for the easy vacuum reducibility of "as-prepared" CZn systems.

3. UV-Vis-NIR DIFFUSE REFLECTANCE SPECTRA

The effects on CZ1.0 samples of the thermal and/or chemical treatments dealt with in the previous sections have been followed also by *in situ* measurements in the UV-Vis-NIR spectral range, and some of the results are reported in **Fig. 15**. With reference to the spectrum of pure ZrO_2 (reported in Fig. 15 as curve 1; the spectrum presents only a strong signal at ~220 nm due to the Zr^{4+}-O^{2-} charge transfer (C.T.)), it is noted that the spectrum of the "as-prepared" sample CZ1.0(300) (curve 2 in Fig. 15) contains a strong signal at ~270 nm, mainly ascribable to the Cu^{2+}-O^{2-} C.T., and a weak broad signal centered at ~750-800 nm, ascribable to d-d transitions of Cu^{2+} ions in octahedral coordination. This spectrum is consistent with the hypothesis that, on the starting catalyst, most of the copper is in the form of dispersed 6-coordinated Cu^{II} species (23). It is recalled that no Cu^{I} species can be revealed, if present, due to the d^{10}

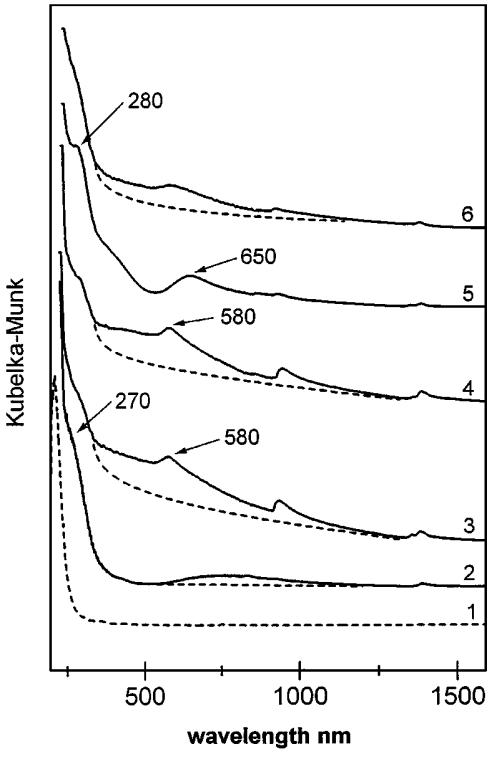

FIG. 15. UV-Vis-NIR reflectance spectra of a Z reference sample and of a CZ1.0 sample treated *in situ* in various conditions: (**1**) (broken line): reference Z(773); (**2**) CZ1.0(300); (**3**) CZ1.0(773); (**4**) After 3, CZ1.0(773) was thoroughly rehydrated at ~300 K, and the excess water evacuated at the same temperature; (**5**) after (3), CZ1.0(773) was oxidized with O_2 (60 torr) at 773 K; (**6**) $CZ1.0(773)_{II}$, i.e., after (3), CZ1.0(773) was oxidized at 773 (as in (5)) and rehydrated at ~300 K (as in (4)), and then the sample underwent a second vacuum activation at 773 K.

configuration. For this reason, no other spectra of CZ1.0 samples activated at temperatures in the 400–700 K range are reported, as in this activation range most of the surface copper reaches the Cu^I state.

Curve 3 of Fig. 15, relative to the CZ1.0(773) sample, presents some remarkable differences, among which most significant are: (i) an appreciable growth of the spectral background in the whole 350–1250-nm range, as evidenced by the broken line; (ii) the formation of a discrete peak at ∼580 nm "on top" of the unresolved intense background. Both observations are indicative of the formation of small particles of reduced metallic copper (Cu^0) and represent the spectroscopic counterpart of the strong darkening observed on the CZ*n* catalysts, further, to a vacuum activation at $T_{act} > 573$ K. In fact it is reported in the literature that the reduction of copper to the Cu^0 state is accompanied by the appearance of strong and often unresolved absorptions in the 300–900-nm range (46), where a broad absorption is assigned to an optical conduction band due to the nucleation of metallic copper. Moreover, the appearance of a discrete absorption at ∼580 nm is to be assigned to a plasmon peak of Cu^0 clusters of increasing size (47,48), as a band at ∼560 nm has been attributed to collective oscillations of free electrons in metallic copper particles. The reduction to the metallic state of a large fraction of copper present at the surface of an "as-prepared" catalyst by the effect of a vacuum treatment at relatively low temperatures is thus confirmed.

Curve 4 of Fig. 15 shows that no appreciable changes are produced in the UV-Vis spectrum by the addition to CZ1.0(773) of excess water. EPR and IR data indicated that the addition of water reoxidises Cu^I species to Cu^{II}, whereas this UV-Vis spectral datum indicates that water has no effect on the particles of Cu^0 that were produced by vacuum thermal reduction.

Curve 5 of Fig. 15 is relative to a CZ1.0(773) sample that has been oxidised *in situ* at 773 K with excess O_2. The high spectral background that was produced in the 350–1250-nm spectral range by the thermal treatment at high temperature has now disappeared. This is the spectroscopic counterpart of the clearing-up observed on reduced CZ samples after a high temperature oxidation step and monitors the oxidative elimination of Cu^0 species. Other features produced in the spectrum are (i) an appreciable intensification of the band at ∼270 nm, ascribed to a Cu^{2+} - O^{2-} C.T. that monitors a fair increase of concentration of Cu^{II} species; (ii) the formation of a broad and asymmetric band centered at ∼650 nm that can be thought of as indicative of the formation of bulk-like CuO particles. In fact, both bulk copper oxide and CuO mechanically diluted in alumina have been reported to be characterised by a strong asymmetrical band centered at ∼620 nm (49). The formation of bulk-like CuO particles, that are known to be EPR silent (41), is thus consistent with the incomplete restoration of the Cu^{II} EPR signal, further, to an oxidation at high temperature.

Curve 6 of Fig. 15, relative to a second vacuum thermal treatment at 773 K carried out on the reoxidized sample of curve 5, indicates that the reduction of Cu^{II} species occurs again, as monitored by a fair decrease of the C.T. band at ∼280 nm (and previously indicated by EPR data), whereas the formation of Cu^0 is not as abundant as it was during the vacuum thermal treatment of the "as-prepared" catalyst. In fact there is a far more modest increase of the spectral background in the 350–1250-nm range, and also, the plasmon band at ∼580 nm is far less evident after the second vacuum treatment at 773 K. These data seem to confirm that Cu^{II} species at the surface of a plainly reoxidized CZ1.0(773) catalyst are still easily reducible to Cu^I (both by a vacuum thermal treatment and by the ambient temperature contact with CO), but are far less reducible to Cu^0 species.

The spectral and redox behaviour typical of "as-prepared" CZ catalysts can be reproduced only if the oxidation treatment at 773 K is followed by a thorough rehydration (at RT, or higher). In that case, and only in that case, the UV-Vis spectrum of the starting CZ1.0(300) sample shown in curve 2 of Fig. 15 is reproduced. This implies that the dispersion of the Cu^{II} species becomes modified by the rehydration process, and in fact, the band at ∼650 nm, due to CuO bulk particles, is eliminated. Thermal treatments *in vacuo* of this oxidised-and-hydrated material will cause changes of the oxidation state of surface copper that are at all similar to those described for the "as-prepared" catalyst, with some differences (not described in detail) that can be ascribed to the fact that the oxidised-and-hydrated catalyst is a "clean" system (i.e., not contaminated by pyrolizable surface hydrocarbonaceous residues; a less pronounced reducibility at $T \geq 573$ K is thus justified).

4. REACTIVITY IN N_2O DECOMPOSITION

As recent works indicate that ZrO_2 itself is active in N_2O decomposition (50–52), preliminary tests were carried out to determine the catalytic role of copper and zirconia. At 723 K the addition of 1% Cu to ZrO_2 improves the conversion of N_2O from about 11% to 62%, whereas the addition of 4% Cu improves N_2O conversion up to 96%. This clearly indicates that the activity of Cu-ZrO_2 in N_2O decomposition is mainly related to the presence of copper ions. It is recalled that doping ZrO_2 with Mg decreases the conversion to about 4% and with Cr to nearly zero. This confirms that ZrO_2 itself possesses intrinsic activity in N_2O decomposition, although the rate of this reaction is significantly lower with respect to that exhibited when copper ions are present.

The influence of the pretreatment conditions on the reactivity of CZ1.0 catalysts in N_2O decomposition at 723 K is shown in **Fig. 16**. The figure reports the percentage conversion of N_2O versus time on stream, after the start of feeding the 1% N_2O/He mixture. Four different pretreatments

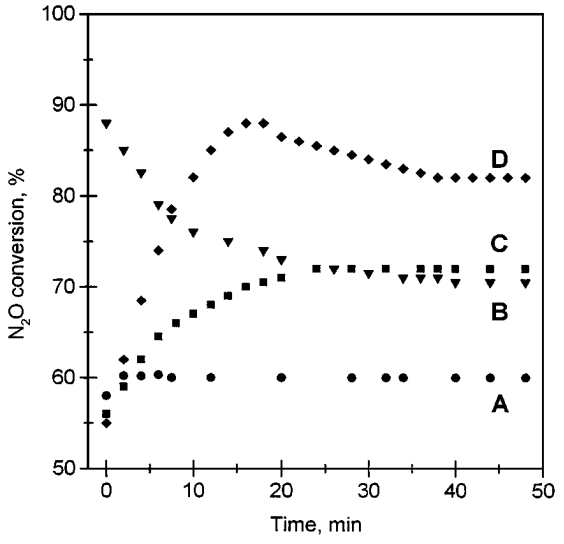

FIG. 16. Reactivity of CZ1.0 samples in N_2O decomposition at 723 K as a function of time on stream and of the type of pretreatment: (**A**) 773 K (1 h) with 20% O_2 in helium; (**B**) 773 K (2h) in helium; (**C**) increase of reactor temperature from r.t. to 723 K in 15 min; and (**D**) treatment at 473 K (15 min) with a flow of 2% H_2O in helium on a sample after pretreatment type (A), followed by an increase of the reactor temperature to 723 K in 10 min in a helium flow. The time on stream equal to zero corresponds to the starting time at which a mixture of 1% N_2O in helium is fed to the reactor.

have been carried out on the same "as-prepared" sample, and namely: (i) pretreatment **A**, consisting of an oxidative activation (1 h at 773 K in a flow of 20% O_2/He); (ii) pretreatment **B**, simulating a high temperature vacuum activation (2 h at 773 K in pure He flow); (iii) thermal pretreatment **C**, consisting of a rapid increase (∼15 min) of the reaction temperature from RT to 723 K in a He flow; (iv) pretreatment **D**, consisting of an *in-situ* rehydration of the catalyst (15 min at 473 K in a flow of a 2% H_2O/He mixture), following the oxidative pretreatment A. After the rehydration step, the reactor temperature was rapidly increased to 723 K (∼10 min).

The plots reported in Fig. 16 show that the pretreatment conditions influence both the stationary activity reached by the catalyst and the transient change of reactivity leading to the stationary behaviour. The catalyst that underwent the oxidative pretreatment A gives the worst results in terms of stationary activity, and the stationary level of N_2O conversion is reached immediately after switching to the 1% N_2O/He feed. All of the other samples reach a stationary activity in about 1 h, although showing different trends. After the mildly reductive pretreatment B the catalyst shows a progressive decline of N_2O conversion activity down to the stationary activity. If the catalyst pretreatment is the simple rapid heating in a He flow up to the reaction temperature (treatment C), the stationary activity reached is comparable to that of the more severe treatment B, but the activity increases to that level, instead of decreasing to it. When the catalyst is rehydrated after a preliminary oxidative treatment (treatment B), the best stationary catalytic activity is observed, and the reactivity passes through a transient maximum.

After reaching the stationary activity, a stable catalytc behaviour lasting at least 1–2 h was observed, although in longer term experiments minor changes were observed, especially in not rehydrated samples, due to minor water and oxygen contamination in the feed. When some 2% H_2O and some 5% O_2 was present with N_2O in the feed, catalytic activity at 573 K was observed to be constant for at least 200 h on stream, even if catalyst activity was shown to be reversibly depressed by the presence of these molecules in the feed (26).

5. FEATURES AND REDOX BEHAVIOR OF COPPER SITES ON ZIRCONIA

Reactivity tests of Cu-ZrO_2 in N_2O decomposition after different pretreatments (Fig. 16) pointed out that both stationary activity and the trend towards stationary activity depend severely on the pretreatment conditions, as do other features evidenced by the spectroscopic characterization of the catalyst.

The different redox states attained by copper at the zirconia surface upon thermal and chemical treatments are schematically summarised below.

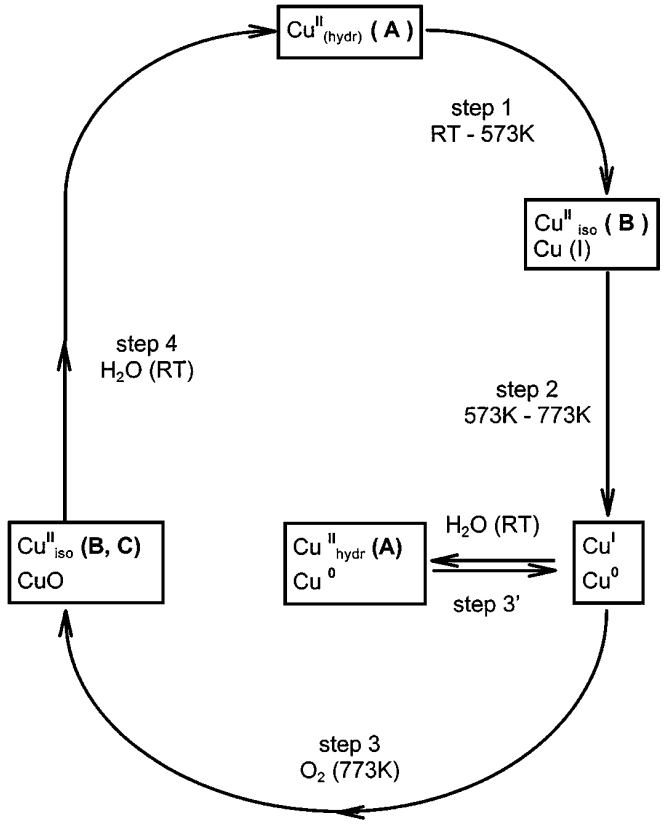

The Cu^{II} species detected by EPR are evidenced in the scheme by the labels used in Table 1 (A, B, C). All other copper species, including CuO particles, are EPR silent. The reduction of Cu^{II} ions by simple outgassing even in rather mild conditions (often incorrectly called autoreduction) has been observed in all experiments of the present work, and follows a stepwise mechanism involving first the reduction to Cu^{I} (step 1) and, for higher outgassing temperatures, a further reduction of a fraction of Cu^{I} or Cu^{II} to Cu^{0} (step 2). Reduction to Cu^{0} is favoured when the oxidised material is in a hydrated form and less pronounced when starting from a hydroxyl-free oxidised surface.

Also the presence of $(CH)_n$ surface contaminants, particularly abundant on the starting materials, plays an important role in the reduction of surface Cu. The reoxidation of the system has been obtained using two different reagents: molecular oxygen and water. Surprisingly, water turns out to be much more effective than oxygen in copper reoxidation; this is obtained at RT using H_2O, whereas high temperatures (773 K) are needed to achieve a comparable copper reoxidation by O_2. The oxidative action of water, however, is limited to Cu^{I} and is not effective on Cu^{0} (step 3′), while the high temperature oxidation by oxygen involves both types of reduced copper (step 3) and leads to the formation of a certain amount of surface dispersed CuO nanoparticles. In these conditions the interaction between the cupric phases and the support is at a maximum and little portions of ZrO_2 surface turn out to be Cu-free. The final hydration (step 4) transforms the isolated copper species in hydrated ones (A) and, since the intensity of the EPR spectra increases to levels even higher than those of the "as-prepared" materials, disaggregation of CuO nanoparticles leads to an increased amount of hydrated Cu^{II} ions. The different concentration of Cu^{II} species between "as-prepared" and oxidized/rehydrated catalysts should be ascribed to the high concentration of carbonate contaminants in the starting materials. These species are rather different from those typical of pure ZrO_2 (53, 54) and far more resistant to evacuation and must, thus, involve Cu surface species. The only hypothesis consistent with EPR, IR, and UV-Vis data is that carbonates, formed during the preparation-cooling phase of the starting materials, stabilizes some Cu surface species in the +1 valence state. Cu^{I} species can be revealed only by IR of CO adsorption, but the Cu^{I} species on "as-prepared" systems cannot interact with CO (either at RT or at 77 K) because strongly held carbonates render the species coordinative saturated.

The so-called "autoreduction" of Cu^{II} is a well-known phenomenon observed for various oxide-supported or zeolitic copper systems, whereas the reoxidation of reduced copper by low temperature interaction with water is less frequently reported, and for zeolitic systems only. Conflicting evidences and interpretations are present in the literature about this phenomenon. In some instances the need for both water and oxygen (even in small amounts) has been claimed as necessary to reoxidize reduced copper (55), whereas other authors indicate, as we have found in the present work, that water alone can oxidize Cu^{I} to Cu^{II} (56).

On the basis of different experimental evidences, two are the chemical pathways discussed in the literature for the reduction–reoxidation of cupric ions by thermal treatment in vacuo (or in an inert gas stream), and both have been proposed to explain the behaviour of Cu/zeolite systems. The first mechanism involves the loss of water and oxygen (55, 57) according to Eq. [1],

$$\begin{aligned} 2[Cu\ OH]^{+} &\leftrightarrow Cu^{2+}\ O^{2-}\ Cu^{2+} + H_2O \\ &\leftrightarrow Cu^{+} \square\ Cu^{+} + \tfrac{1}{2}O_2, \end{aligned} \qquad [1]$$

where the starting cupric ions are written in the hydroxylated form present in hydrated zeolites and the symbol □ represents a vacancy of "extralattice oxygen" (as no oxygen can be lost by the zeolitic framework (58)). The extralattice oxygen can be eliminated either by desorption at high temperature, as proposed by Iwamoto *et al.* (57, and references therein) and as indicated in Eq. [1], or by the action of a reducing agent (namely CO), as reported by Vaylon *et al.* (58). A second mechanism, exclusively based on water elimination, has been proposed by Bell and co-workers (56) on the basis of EPR data and is based on a complex pathway involving the formation of hydroxyl radicals in their usual form ($OH^{\bullet}$) and in the deprotonated form (O^{-} ions):

$$\begin{aligned} Cu^{2+}\ OH^{-} &\leftrightarrow Cu^{+} + OH^{\bullet} \\ Cu^{2+}\ OH^{-} + OH^{\bullet} &\leftrightarrow Cu^{2+}\ O^{-} + H_2O \\ \hline 2[Cu^{2+}\ OH^{-}] &\leftrightarrow Cu^{+} + Cu^{2+}\ O^{-} + H_2O \end{aligned} \qquad [2]$$

According to this mechanism a fraction of copper is actually reduced to Cu^{I} while a second (equivalent) fraction remains as Cu^{II} in the form of a Cu^{2+} - O^{-} pair, undetectable by EPR. The addition of water would restore the initial oxidation state. It is worth mentioning that the two oxygen radical species reported in the above mechanism have not been directly observed by the authors.

As for the redox chemical cycle observed in the present work, the reduction of Cu^{II} ions brought about by thermal treatments (steps 1 and 2 in the previous scheme) is likely to be favoured by the nature of the zirconia support which is, *per se*, able of losing molecular oxygen, giving rise to reduced Zr^{3+} surface centers (59). In the case of Cu-ZrO_2 systems, Cu^{II} ions would be the preferential electron scavenger centers. The role of oxygen depletion from the support is also indirectly indicated by the easy formation of thoroughly reduced Cu^{0} particles which is not observed, under similar conditions, in zeolitic systems.

The mechanism of reoxidation by water vapour (step 3′) remains rather puzzling. Our data differ from those of Kasai

and Bishop (55), who claim that the joint action of water and oxygen is needed to observe reoxidation of reduced copper mordenites, and are in line with the results of Bell and coworkers (56), who observe that water alone is capable of oxidizing Cu^{I} to Cu^{II} at room temperature. Still, the mechanism of Eq. [2] (53) is not completely convincing, in that the formation of a hydroxyl radical ($OH^{\bullet}$) on a hydrated surface is not highly probable in the present experimental conditions and should be demonstrated. The complete understanding of the oxidative action of water on Cu^{I} ions is thus left to further experimental investigations aimed at clarifying the following points: (i) the presence and the possible role of traces of oxygen in the water vapour put in contact with the samples (in the present work, multiple distillation of water did not produce any change); (ii) the possible onset of a radical chemistry such as that described in Ref. (56); (iii) the possible formation of H_2 upon contact of water with the reduced catalyst, indicating the reduction of water hydrogen. This latter point has been already addressed by Kasai and Bishop (55) for Cu and Cr exchanged mordenite. They showed that the reduction of water hydrogen indeed occurs in the case of Cr samples and does not occur in the case of Cu samples. They explained the difference in terms of standard redox potentials, although the conditions for redox reactions at the surface of a complex heterogeneous system (or in a zeolitic framework) are very far from those corresponding to a *standard* electrochemical cell; the possible evolution of the reaction in the direction opposite to that indicated by the standard potentials cannot be ruled out.

In order to check this hypothesis and verify the possible formation of H_2 by contacting water with "autoreduced" Cu-ZrO_2 the following experiments were made: CZ1.0 was pretreated in a quartz reactor at about 773 K in a nitrogen flow for 1 h and, then, after cooling to 343 K (still in the nitrogen flow), water was added to the nitrogen flow by means of an infusion pump so as to make a step-change in water concentration from 0 to about 3%. Using a mass-quadrupole detector the reactor outlet was continuously monitored in real-time. In order to better show the formation of hydrogen, D_2O was used, because the background values for mass 4 (D_2) and 3 (HD) are lower than for mass 2 (H_2) and, thus, the detection of HD or D_2 upon contact of D_2O with a pretreated catalyst should be easier. No evidence for the formation of HD or D_2 after the addition of D_2O to the nitrogen flow was ever found. Similar results were observed also when, with D_2O, also some 2% oxygen was added to the nitrogen flow in a step-change mode. Also, a brief catalyst reduction treatment (in 10% H_2/N_2 flow at 573 K for 15 min), followed by cooling to 473 K in pure nitrogen flow did not allow us to detect HD or D_2 after D_2O addition.

The lack of hydrogen formation thus excludes, within detection limits of our tests, that a plain redox mechanism of Cu^{I} reoxidation by water is responsible for the behaviour observed and indicates that more complex phenomena occur at the surface of Cu-ZrO_2 samples. Further studies are obviously necessary to clarify the details of the mechanism by which water vapour does indeed reoxidize Cu^{I} species on ZrO_2 surface.

6. RELATIONSHIP BETWEEN NATURE OF COPPER IONS AND REACTIVITY IN N_2O DECOMPOSITION

The catalytic activity of Cu/ZrO_2 catalysts was shown (Fig. 16) to depend on the oxidation state of copper ions and on the hydration state of the surface.

A purely oxidative pretreatment (A) gives the worst results, due to the formation of CuO particles that are probably inactive in N_2O decomposition. If, after the oxidative pretreatment, the sample is hydrated (treatment D) a fair improvment of the catalyst reactivity is observed. This can be ascribed to the redispersion of copper from CuO particles to isolated Cu^{2+} species (caused by rehydration; step 4 of the scheme), followed by reduction to isolated Cu^{+} ions in the final part of the treatment (step 1 of the scheme). Moreover, the elimination of surface contaminants favours a better dispersion of Cu^{2+} ions with respect to "as-prepared" samples and, thus, leads after pretreatment D to a higher stationary activity than after pretreatment B or C. Sample D exhibits a growth of activity and a relative maximum before reaching stationary behaviour. As after the oxidative pretreatment this sample underwent a rapid increase of temperature under inert gas up to the temperature of the catalytic tests (723 K), it is thought that the catalytic response is due to a gradual transformation of surface copper species:

$$Cu^{2+}\text{-}OH_2 \rightarrow Cu^{+}\text{-}OH_2 \rightarrow Cu^{+}_{\text{hydrox.}} \rightarrow Cu^{+}_{\text{dehydrox.}}.$$

The maximum activity would be thus due to Cu^{+} species in a more hydrated form.

Pretreatments B and C (high and low temperature pretreatment in He) leads to the same stationary activity, lower than in case D. This is probably a consequence of the "cleaner" surface obtained with treatment D and of a better dispersion of copper ions. On the other hand, the nonoxididative pretreatment at high temperature (B) is likely to lead to the formation of significant amounts of Cu^{0}, due to the presence of surface hydrocarbonaceous contaminants. On the contrary, in the nonoxidative pretreatment at lower temperature (case C) Cu^{0} species should not form. The presence in case B of Cu^{0} species is likely to be responsible for the high initial activity of the catalyst, as the activity of Cu^{0} species in N_2O is known (14). When reoxidation of Cu^{0} by N_2O to form CuO particles is complete, the residual activity is only due to the presence of isolated Cu^{+} species: also these species are reoxidized during N_2O decomposition, possibly by reaction of N_2O with O^{*} surface oxygen

species to give $N_2 + O_2$ and with simultaneous oxydation of Cu^+, as indicated by Kapteijn *et al.* (44,60). Cu^{II} species so formed can spontaneously reduce again at the temperature of the catalytic tests (see step 1 of the scheme). The presence in B of lower amounts of isolated Cu^I species with respect to case D explains the lower stationaryk activity.

Finally, in case C the less severe thermal conditions of the nonoxidative pretreatment avoid the formation of Cu^0 particles and thus justify the absence of the initial higher activity and successive decline, typical of case B.

CONCLUSIONS

Catalytic activity of Cu-ZrO_2 systems turns out to be highly sensitive to the pretreatment of the solid and to the state of hydration/oxidation of the surface. The main features of the system are as follows:

(i) The catalyst is an efficient redox system in that the redox state of the active Cu phase undergoes strong changes even in mild reductive or oxidative conditions. In particular, the "autoreduction" of Cu^{II} is very pronounced in mild conditions of thermovacuum treatment, as it is assisted by the zirconia matrix which is capable of oxygen depletion.

(ii) Two different families of isolated copper ions have been detected both by EPR (Cu^{II} centres) and IR (Cu^I centres). The Cu^{II} centres have an axial symmetry (likely of distorted octahedral type), and both types of Cu sites are coordinatively unsaturated.

(iii) The reduction of the system to Cu^0 is more effective when the starting material is surface hydrated and when in the presence of hydrocarbonaceous contaminants. A dehydrated and/or "clean" material preferentially leads to Cu^I formation.

(iv) Water adsorption at room temperature efficiently oxidizes Cu^I to Cu^{II}, whereas O_2 at high temperature is needed to oxidize Cu^0. The mechanism of the former process is not yet fully understood. The oxidation of Cu^0 (by O_2 or N_2O at relatively high temperatures) leads to CuO nanoparticles, whose Cu^{II} ions are redispersed at the surface by water adsorption.

(v) Only the joint action of high-temperature oxidation and ambient temperature hydration reproduces the conditions of Cu^{II} on the starting Cu-ZrO_2 systems. The maximum surface concentration of dispersed Cu^{II} centres is obtained through the oxidation–hydration process, due to the role played by surface contaminants, abundantly present on the starting materials. After a complete reduction–oxidation–rehydration cycle, as well as on the starting materials, Cu^{II} ions are similar to those observed on several hydrated systems; the coordination sphere of the ions is virtually complete and is made of oxide ions of the solid and of hydroxy groups and/or coordinated water molecules.

(vi) The stationary and nonstationary catalytic behaviours in N_2O decomposition depend significantly on the type of catalyst pretreatment, as the pretreatment determines the presence/amount of surface contaminants and the hydration state of the surface. Both factors are important in determining the redox behaviour of copper ions at the ZrO_2 surface.

REFERENCES

1. Sohn, J. R., Cho, S. G., Pae, Y., and Hayashi, S., *J. Catal.* **159**, 170 (1996).
2. Indovina, V., Occhiuzzi, M., Ciambelli, P., Sannino, D., Ghiotti, G., and Prinetto, F., *in* "11th International Congress on Catalysis—40th Anniversary" (J. W. Hightower, W. N. Delgass, E. Iglesias, and A. T. Bell, Eds.), Stud. Surf. Sci. Catal., Vol. 101, p. 691. Elsevier Science, Amsterdam, 1996.
3. Boot, L. A., van Dillen, A. J., Geus, J. W., and van Baren, F. R., *J. Catal.* **163**, 195 (1996).
4. Chen, K., Fan, Y., Hu, Z., and Yan, Q., *Catal. Lett.* **36**, 139 (1996).
5. Kim, D. S., and Wachs, I. E., *J. Catal.* **142**, 166 (1993).
6. Kim, D. S., Wachs, I. E., and Segawa, K., *J. Catal.* **146**, 268 (1994).
7. Pratt, K. C., Sanders, J. V., and Chistov, V., *J. Catal.* **124**, 416 (1990).
8. Hamon, D., Vrinat, M., Breysse, M., Durand, B., Jebrouni, M., Roubin, M., Magnaix, P., and Des Courieres, T., *Catal. Today* **10**, 613 (1991).
9. Boot, L. A., Kerkhoffs, M. H., van der Linden, B. Th., van Dillen, A. J., Geus, J. W., and van Buren, F. R., *Appl. Catal. A: General* **137**, 69 (1996).
10. Ali, S., Chen, B., and Goodwin, J. G., *J. Catal.* **157**, 35 (1995).
11. Mark, M. F., and Maier, W. F., *J. Catal.* **164**, 122 (1996).
12. Borer, A. L., Brönnimann, C., and Prins, R., *J. Catal.* **145**, 516 (1994).
13. Burch, R., and Loader, P. K., *Appl. Catal. A: General* **143**, 317 (1996).
14. Centi, G., and Perathoner, S., *Appl. Catal. A: General* **132**, 179 (1995).
15. Fisher, I. A., Woo, H. C., and Bell, A. T., *Catal. Lett.* **44**, 11 (1997).
16. Denise, B., and Sneeden, R. P. A., *Appl. Catal.* **28**, 235 (1986).
17. Chen, H. W., White, J. M., and Ekerdt, J. G., *J. Catal.* **99**, 293 (1986).
18. Koeppel, R. A., Baiker, A., and Wokaum, A., *Appl. Catal. A: General* **84**, 77 (1992).
19. Sun, Y., and Sermon, P. A., *Catal. Lett.* **29**, 361 (1994).
20. Delahay, G., Coq, B., Ensuque, E., and Figueras, F., *Catal. Lett.* **39**, 105 (1996).
21. Bethke, K. A., Alt, D., and Kung, M. C., *Catal. Lett.* **25**, 37 (1994).
22. Bethke, K. A., Li, C., Kung, M. C., and Kung, H. H., *Catal. Lett.* **31**, 287 (1994).
23. Okamoto, Y., Gotoh, H., Aritani, H., Tanaka, T., and Yoshida, S., *J. Chem. Soc., Faraday Trans.* **93**, 3879 (1997).
24. Dow, W.-P., and Huang, T.-J., *J. Catal.* **160**, 171 (1996).
25. Dow, W.-P., and Huang, T.-J., *J. Catal.* **147**, 322 (1996).
26. Centi, G., Cerrato, G., D'Angelo, S., Finardi, U., Giamello, E., Morterra, C., and Perathoner, S., *Catal. Today* **27**, 265 (1996).
27. Li, Y., and Armor, J. N., *Appl. Catal. B: Environmental* **1**, L21 (1992).
28. Li, Y., and Armor, J. N., U.S. Patent 5,171,553 (1992).
29. van Amstel, A. R., and Steward, R. J., *Fert. Res.* **37**, 213 (1994).
30. Kroeze, C., *Sci. Tot. Environ.* **152**, 189 (1994).
31. De Soete, E., *Rev. Inst. Fr. Petrol.* **48**, 4123 (1993).
32. Centi, G., Perathoner, S., Cerrato, G., Giamello, E., and Morterra, C., *in* "Proceedings, 11th International Congress on Catalysis—40th Anniversary, Baltimore, MD, July 1996," pg. 135.
33. Liu, Z., Ji, W., Dong, L., and Chen, Y., *J. Catal.* **172**, 243 (1997).
34. Berger, P. A., and Roth, J. F., *J. Phys. Chem.* **71**, 4307 (1967).
35. Centi, G., Perathoner, S., Biglino, D., and Giamello, E., *J. Catal.* **152**, 75 (1995).

36. Giamello, E., Murphy, D., Magnacca, G., Morterra, C., Shioya, Y., Nomura, T., and Anpo, M., *J. Catal.* **136**, 510 (1992).
37. Sheppard, N., and Nguyen, T. T., *Adv. Infrared Raman Spectr.* **5**, 67 (1978).
38. Morterra, C., Cerrato, G., Bolis, V., Lamberti, C., Ferroni, L., and Montanaro, L., *J. Chem. Soc. Faraday Trans.* **91**, 113 (1995).
39. Morterra, C., Cerrato, G., Ferroni, L., and Montanaro, L., *Mater. Chem. Phys.* **37**, 243 (1994).
40. Davydov, A. A., "Infrared Spectroscopy of Adsorbed Species on the Surface of Transition Metal Oxides" (C. H. Rochester, Ed.), Wiley, New York, 1984.
41. Lumbeck, H., and Voitländer, F., *J. Catal.* **13**, 117 (1969). [Giamello, E., Fubini, B., Lauro, P., *Appl. Catal.* 21, 133 (1986)]
42. Busca, G., and Lorenzelli, V., *Mater. Chem.* **7**, 89 (1982).
43. Hadjiivanov, K. I., Kantcheva, M. M., and Klissurski, D. G., *J. Chem. Soc., Faraday Trans.* **92**, 4595 (1996).
44. Kaptejin, F., Mul, G., Marban, G., Rodriquez-Mirasol, J., and Moulijn, J. A., *in* "Proceedings, 11th International Congress on Catalysis—40th Anniversary" (J. W. Hightower, W. N. Delgass, E. Iglesia, and A. T. Bell, Eds.), p. 641. Elsevier Science, Amsterdam, 1996.
45. Miessner, H., Landmesser, H., Jaeger, N., and Richter, K., *J. Chem. Soc., Faraday Trans.* **93**, 3417 (1997).
46. Coudurier, G., Decamp, T., and Praliaud, H., *J. Chem. Soc., Faraday Trans.* **78**, 2661I (1982).
47. Lisiecki, L., and Pileni, M. P., *J. Phys. Chem.* **99**, 5077 (1995).
48. Yanase, A., and Komiyama, H., *Surf. Sci.* **248**, 11 (1991).
49. Marion, M. C., Garbowski, E., and Primet, M., *J. Chem. Soc., Faraday Trans.* **86**, 3027 (1990).
50. Lin, J., Chen, H. Y., Chen, L., Tan, K. L., and Zeng, H. C., *Appl. Surf. Sci.* **103**, 307 (1966).
51. Miller, T. M., and Grassian, V. H., *Colloid Surface A* **105**, 113 (1995).
52. Miller, T. M., and Grassian, V. H., *J. Am. Chem. Soc.* **117**, 10969 (1995).
53. Morterra, C., and Orio, L., *Mater. Chem. Phys.* **24**, 247 (1990).
54. Morterra, C., Cerrato, G., and Ferroni, L., *J. Chem. Soc. Faraday Trans.* **91**, 125 (1995).
55. Kasai, P. H., and Bishop, R. J., *J. Phys. Chem.* **81**, 1527 (1977).
56. Larsen, S. C., Aylor, A., Bell, A. T., and Reimer, J. A., *J. Phys. Chem.* **98**, 11533 (1994).
57. Iwamoto, M., Yahiro, H., Tenda, K., Mizuno, N., Mine, Y., and Kagawa, S., *J. Phys. Chem.* **95**, 3727 (1991).
58. Vaylon, J., and Keith Hall, W., *J. Phys. Chem.* **97**, 7054 (1993).
59. Morterra, C., Giamello, E., Orio, L., and Volante, M., *J. Phys. Chem.* **94**, 3112 (1990).
60. Kapteijn, F., Marbàn, G., Rodriguez-Mirasol, J., and Moulijn, J. A., *J. Catal.* **167**, 256 (1997).